Impacts of Differing Melt Regimes on Satellite Radar Waveforms and Elevation Retrievals

We would like to thank Anonymous Reviewer 1 for a thoughtful and insightful review of our manuscript and appreciate all the feedback. Below, we have included responses to the points raised.

The introduction needs to be improved. It makes sense to supplement the rationale of performing this kind of research.

Thank you for raising this issue. The revised manuscript contains background that has been merged with the introduction, and additional justification has been added to the paper. We also added relevant information regarding the ULI and OCOG retracker (including equations). In general, this study addresses resulting questions from Nilsson et al. 2015. through the creation of a framework to calculate and evaluate Level 1B Baseline D LeW and Level 2 elevation time series at any given location on the GrIS within CryoSat-2's LRM zone (Ronan et al., 2024).

Have you tried Baseline-E for the LeW and I wonder if there is any difference between the two datasets?

We have looked at CryoSat-2's Baseline-E documentation when performing this study, although it was never applied to this specific study. Relevant to our study, Baseline – E improves upon the Level 2 Slope Correction algorithm in the Land-Ice Retracker (Exprivia, 2021). This change is noted to change the Level-2 elevations (and importantly, not Level 1B waveforms) on the order of magnitude of a cm (Exprivia, 2021). Given the Level -2 elevations derived at NEEM and Summit Station exceed this threshold, we felt comfortably continuing our work in Baseline-D, which was originally chosen to continue the work of Nilsson et al. 2015.

Figure 2: could you please also mark the boundary of the dry snow zone and percolation zone to make it easier for the readers to cross-reference the area in the manuscript?

This is an excellent comment, and one that was a guiding question of the corresponding author when developing his MS studies proposal. The original distinctions between dry snow, percolation, and ablation zones along the Greenland Ice Sheet (GrIS) were first described by Benson in 1962 based on ground surveys (Benson, 1996) and further in Partington et al. 1989, although it is currently something up for debate (Rizzoli et al., 2017). Given that the melting regime constantly change as a factor of meteorological and climatological processes, the boundary is not static – and would not be possible to label in this paper. On a more pedantic level given a changing climate, are these zone – labels still appropriate for the GrIS? A future paper could potentially investigate using LeW from CryoSat-2 to create an entirely new classification,

since we see different responses based on the current regime classifications. We added wording to the Figure 3 captions to indicate what melt regime (based on the Benson classification).

The methodology is oversimplified without providing technical details. For example, how do you filter the invalid waveforms and how to derive the time series? I suggest the authors add a flowchart of the developed approach in methodology.

We agree with your assessment that the original methodology section was oversimplified and did not contain enough technical details. While we did not include a flowchart in the updated methodology (Section 2 of the Revised Manuscript), we included six new subsections which include information on the workflow used. Section 2.2 focuses on the derivation of the time series, and Section 2.4 includes Outlier information, such as how many outliers were removed from each site location (more information (outside of revised manuscript) can be found in Section 4.0 of the Supplement).

Line 60: Because CryoSat-2 also has SIN mode over Greenland, it would be better to clarify that you are focusing on LRM mode in the beginning. As far as I know, OCOG and UCL retrackers are applied to the LRM mode only as per the handbook of Baseline-D.

Agreed. We reworded that specific line in the Revised Manuscript to better address the situation and decrease confusion about the available retrackers. Baseline-D also contains the Ocean CFI retracker (which is labelled #1 in ESA's documentation). The Ocean CFI algorithm is a model-retracker, and uses the Brown-Hayne Model, making it similar in practice to the ULI Retracker. For this study, we focus on the ULI retracker (#2 in the documentation), and the OCOG retracker (#3 in the documentation)

Line 67: Please correct the citation format for (Ferraro & Swift, 1995), (Tourian et al., 2012) because a comma here looks weird.

Thank you for bringing this to our attention. This has been corrected.

Line 134: Please provide some introduction to the Bayesian Estimator for Abrupt Seasonality and Trend (BEAST) algorithm. Why do you choose 1/8 year interval? I wonder what is the sensitivity to the interval (e.g., 1/4 or 1/2 year).

We have included more information on the BEAST algorithm within the methodology component. The BEAST algorithm, in short, uses Bayesian inference and model averaging to avoid the somewhat arbitrary model-picking process (Zhao et al., 2019), especially considering that the CryoSat-2 Level 1B and Level 2 data have irregularly spaced collections. When writing the Python Script, we ran the BEAST algorithm with multiple window lengths (1/2, ¼, 1/8, and 1/12). In examining the results, the outputted trends in all except $1/8^{th}$ contained either a smoothed trend (i.e. remove all signal entirely), or created artificially generated peaks and troughs, likely from the data-interpolation operation. We chose the $1/8^{th}$ window length to minimize these effects. While the BEAST algorithm is designed for irregularly spaced datasets, it was designed originally for data with more collects (i.e. LANDSAT, MODIS) (Zhao et al. 2019). More BEAST information can be found in Section 2.3 of the Revised Manuscript.

I wonder if plotting the LeW as a result of the slope (e.g., from an Arctic dem) or roughness would help explain your finding.

This is an interesting question. While surface roughness can influence the LeW (Ashcraft & Long, 2005; Legrésy & Rémy, 1997), Nilsson et al., 2015 indicates that surface roughness does not seem to be a contributing factor to the medium-long term LeW trend as evidenced by the σ_0. trend series. As such, we do not think that surface roughness would explain this finding. Similarly, the slope at any given site would not change significantly enough (i.e. Summit Station; Hawley et al., 2020) at any given location to generate the LeW trends we've recorded.

Figures 4 and 5: In addition to the time series, could you please also make a climatology plot that shows how the LeW varies for each of the months using all the data during 2010-2022?

We have included graphs that show how the LeW varies for each of the months for each location during the duration of data (Section 5 of the supplement). There is no noticeable trend or pattern in LeW for any given month over the year. This conclusion makes sense to us, since we argue that LeW has other controls, such as melting, etc. If we were able to deconvolve the amount of forcing these controls have on the LeW, it might be possible to separate out specific climatological controls on the LeW. That would be a good foundation for future research.

Line 260: I am interested to see a plot that includes the waveforms with retracked points marked before/after melt (would be good to mark the corresponding locations as well) and you could just select some typical waveforms to better illustrate how the LeW has varies due to the melt.

Thank you for the suggestion! We added two representative Level 1B waveforms from Summit Station – one before the 2012 Melting Event, and one after the melting event, each with the Level 2 OCOG & ULI Retracked locations:

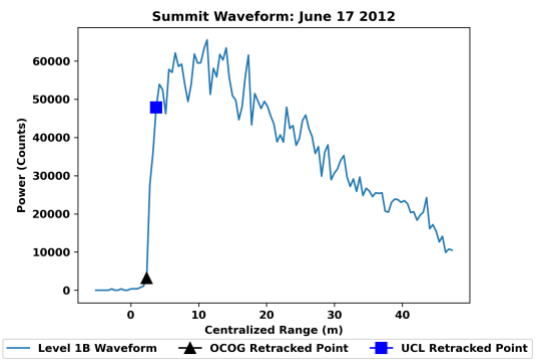

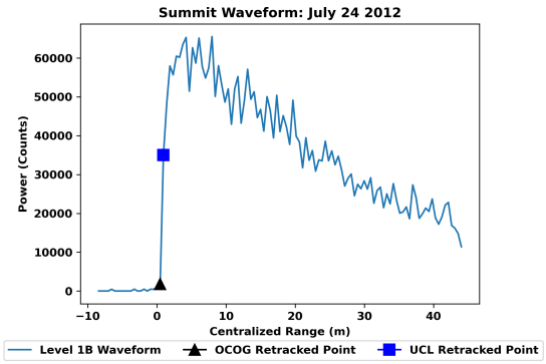

These specific figures can be found in Section 4.1. of the Revised Manuscript

References:

Ashcraft, I. S. and Long, D. G.: Observation and characterization of radar backscatter over Greenland, IEEE Transactions on Geoscience and Remote Sensing, 43, 225–237, https://doi.org/10.1109/TGRS.2004.841484, 2005.

Benson, C. S.: Stratigraphic Studies in the Snow and Firn of the Greenland Ice Sheet, Snow Ice and Permafrost Research Establishment, Corps of Engineers, U.S. Army, Wilmette, Illinois, 1996.

Exprivia: Instrument Processing Facility Baseline E Evolutions, https://earth.esa.int/eogateway/documents/20142/37627/Cryosat-Baseline-E-Evolutions.pdf, last access: July 14, 2024, 2021

Hawley, R. L., Neumann, T. A., Stevens, C. M., Brunt, K. M., and Sutterley, T. C.: Greenland Ice Sheet Elevation Change: Direct Observation of Process and Attribution at Summit, Geophys Res Lett, 47, e2020GL088864, https://doi.org/10.1029/2020GL088864, 2020.

Legrésy, B. and Rémy, F.: Altimetric observations of surface characteristics of the Antarctic ice sheet, Journal of Glaciology, 43, 265–275, https://doi.org/10.3189/S002214300000321X, 1997.

Nilsson, J., Vallelonga, P., Simonsen, S. B., Sørensen, L. S., Forsberg, R., Dahl-Jensen, D., Hirabayashi, M., Goto-Azuma, K., Hvidberg, C. S., Kjær, H. A., and Satow, K.: Greenland 2012 melt event effects on CryoSat-2 radar altimetry, Geophys Res Lett, 42, 3919–3926, https://doi.org/10.1002/2015GL063296, 2015.

Partington, K. C., Ridley, J. K., Rapley, C. G., and Zwally, H. J.: Observations of the Surface Properties of the Ice Sheets by Satellite Radar Altimetry, Journal of Glaciology, 35, 267–275, https://doi.org/10.3189/S0022143000004603, 1989.

Rizzoli, P., Martone, M., Rott, H., and Moreira, A.: Characterization of Snow Facies on the Greenland Ice Sheet Observed by TanDEM-X Interferometric SAR Data, Remote Sensing 2017, Vol. 9, Page 315, 9, 315, https://doi.org/10.3390/RS9040315, 2017.

Ronan, A., Hawley, R., and Chipman, J.: Impacts of Differing Melt Regimes on Satellite Radar Waveforms and Elevation Retrievals: Data & Scripts., Zenodo [dataset], https://doi.org/10.5281/zenodo.10969275, 13 April 2024.

Zhao, K., Valle, D., Popescu, S., Zhang, X., and Mallick, B.: Hyperspectral remote sensing of plant biochemistry using Bayesian model averaging with variable and band selection, Remote Sens Environ, 132, 102–119, https://doi.org/10.1016/J.RSE.2012.12.026, 2013.

Impacts of Differing Melt Regimes on Satellite Radar Waveforms and Elevation Retrievals: Supplemental

Alexander C. Ronan[1], Robert L. Hawley[1], Jonathan W. Chipman[1,2]

[1]Department of Earth Sciences, Dartmouth College, Hanover NH, 03755, United States
[2]Department of Geography, Dartmouth College, Hanover NH, 03755, United States

Correspondence to: Alexander C. Ronan (alexander.clark.ronan@dartmouth.edu)

1.0. Location of Additional Field Sites

We choose Summit Station and Raven to represent locations with differing amounts of surface melt in two melt regimes (Dry Snow and Percolation Zone) (Table 1). The third site, NEEM (Dry Snow Zone), is chosen to compare this study's Level 1B analysis with that of Nilsson et al. (2015). The fourth and fifth sites, 50 km-NEEM and Similar-NEEM, are chosen to be tested to confirm the results of NEEM and to understand the spatial variability of possible melt signature and response in the Level 1B metric time series.

Site	Coordinates (WGS1984)	Avg. Annual accumulation from 1958 – 2019[a] (mm-w.e)	Avg. Annual Snowmelt from 1958 – 2019[a] (mm-w.e)	Elevation[b] (m)
Summit	72.5833, -38.4500	205.50	0.52	3251
NEEM	77.4500, -51.0600	184.45	1.84	2481
50 km-NEEM	77.2005, -49.3120	184.96	1.45	2581
Similar-NEEM	77.6000, -40.0000	93.08	4.10	2523
Raven/DYE-1	66.4964, -46.2849	455.92	151.01	2200

Table 1: Study Sites (Noël et al., 2019[a]; Howat et al., 2015[b])

2.0 Waveform Metrics

2.1. Leading Edge Width (LeW)

Here, we plot LeW for each site in the paper, as well as our additional sites. Though Summit, Neem, and Raven are all shown in the paper, we reproduce them here for completeness and for comparison with the additional two sites.

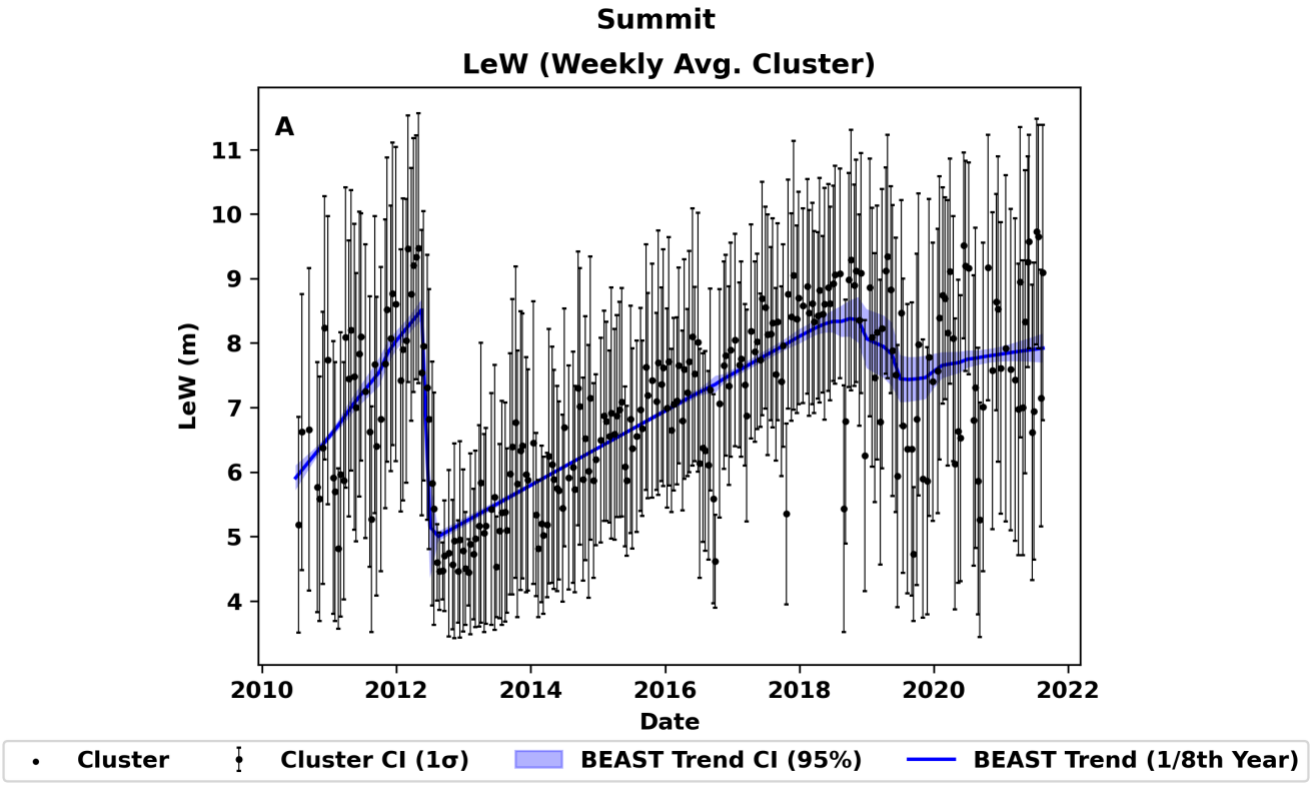

Figure 1A: LeW Trend at Summit Station

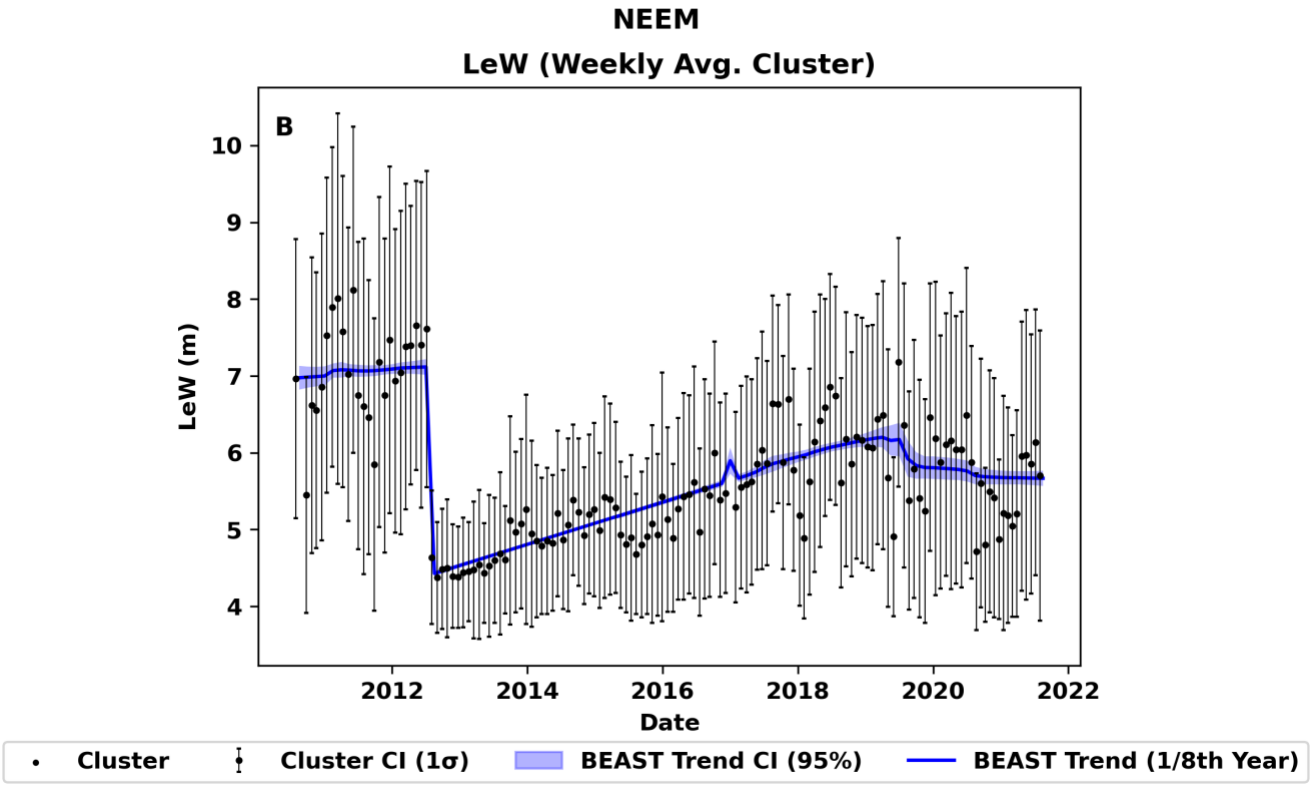

Figure 1B: LeW Trend at NEEM

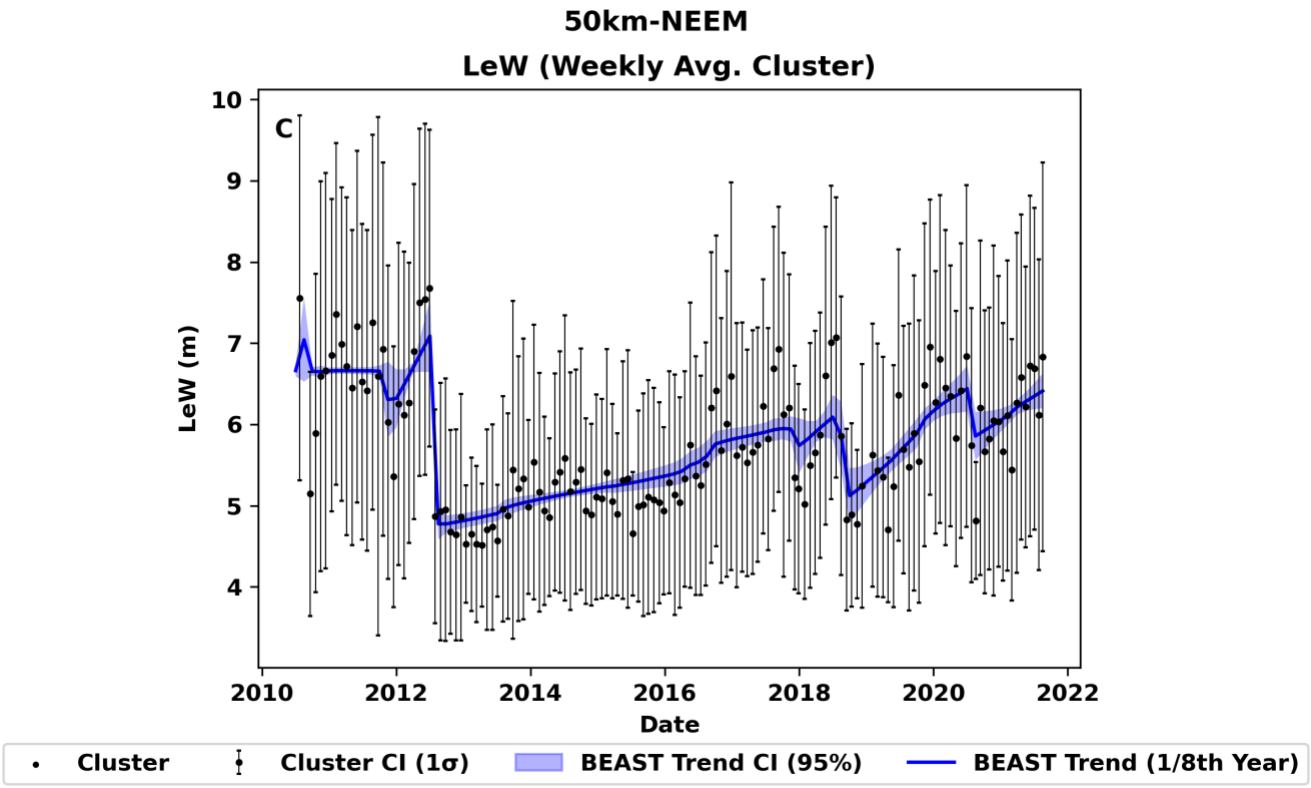

Figure 1C: LeW Trend at 50km-NEEM

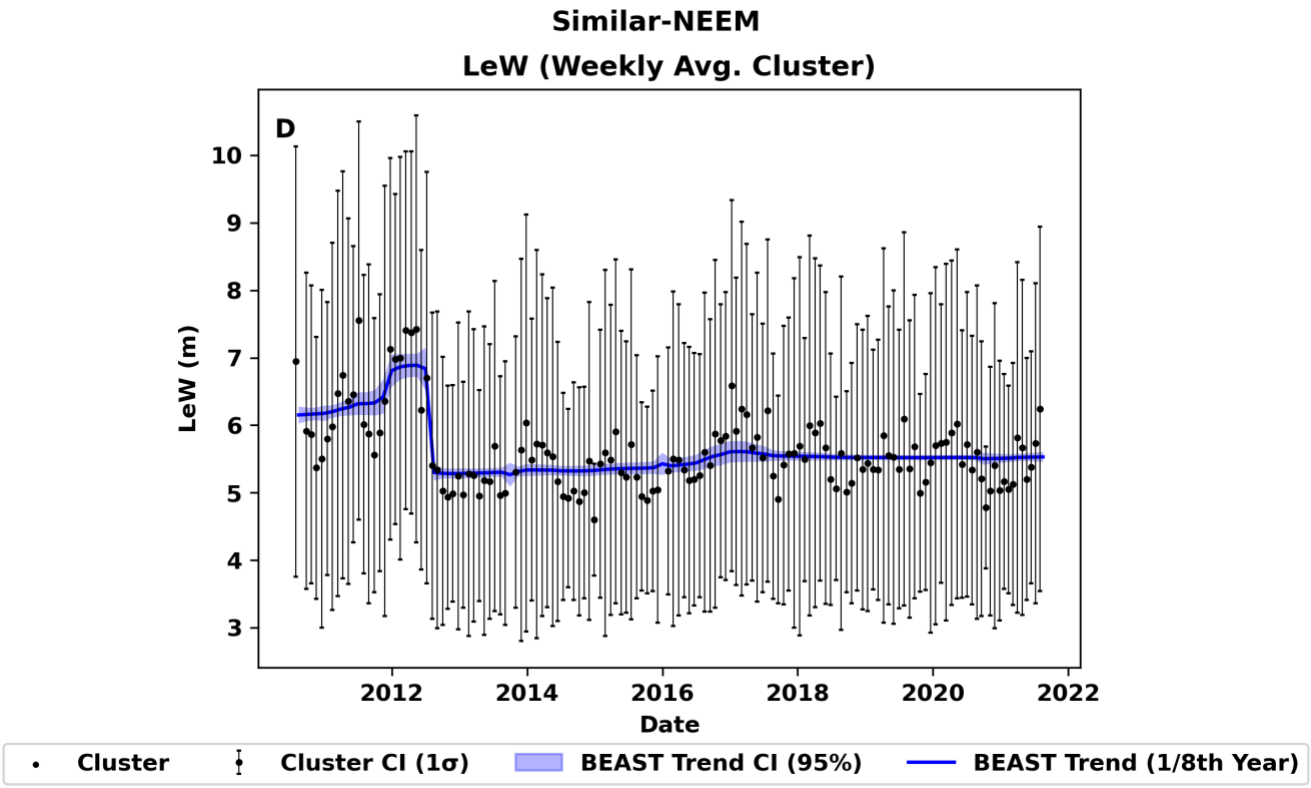

Figure 1D: LeW Trend at Similar-NEEM

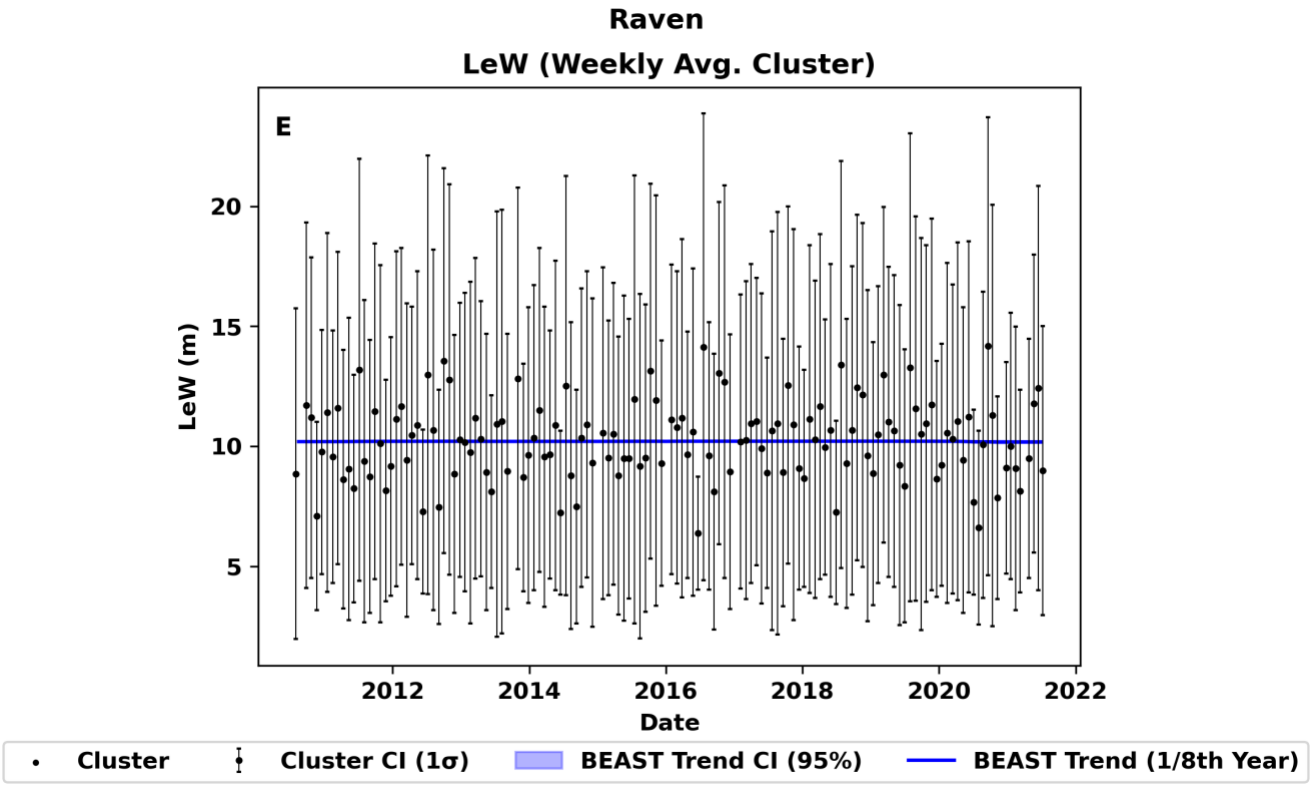

Figure 1E: LeW Trend at Raven

2.2 Riemann's Sum Integral (RSI)

Unlike Level 1B data used in this study to calculate and analyse waveform characteristics, SIRAL Level 2 data contain σ^0 (backscatter coefficient) values derived from each retracking algorithm. σ^0 is defined as the calibrated backscatter cross section of the pulse return (Dawson and Landy, 2023). σ^0 values partly depend on waveform amplitudes defined by the retracking algorithms (European Space Agency, 2019). A Riemann Sum Integral (RSI) is calculated for each returning waveform, as the calibration values used to calculate σ^0 are not known in this study. In this capacity, RSI is equivalent to non-calibrated backscatter.

RSI at Summit (Figure 2A) is negatively correlated with ULI-retracker derived elevations (TTT, α=0.05, r = -0.72, $p < 0.0001$), and correlated with the OCOG-retracker derived elevations (TTT, α=0.05, r = -0.33, p = 0.00058). Similarly, RSI at NEEM (Figure 2B) is negatively correlated with ULI-retracker derived elevations (TTT, α=0.05, r = -0.85, $p < 0.0001$), and correlated with the OCOG-retracker derived elevations (TTT, α=0.05, r = -0.40, p = 0.00005). RSI at Raven (Figure 2E) is neither correlated with ULI-retracker derived elevations (TTT, α=0.05, r = 0.007289, p = 0.94434) or with the OCOG-retracker derived elevations (TTT, α=0.05, r = 0.11896, p = 0.24490).

LeW and RSI are correlated at Summit (TTT, α=0.05, r = 0.79, p = <0.00001), NEEM (TTT, α=0.05, r = 0.57, p = <0.00001) and Raven (TTT, α=0.05, r = 0.60, p = <0.00001). The negative correlations between RSI and ULI-derived Level 2 elevations can be explained by this LeW correlation, which shows that RSI is not calibrated.

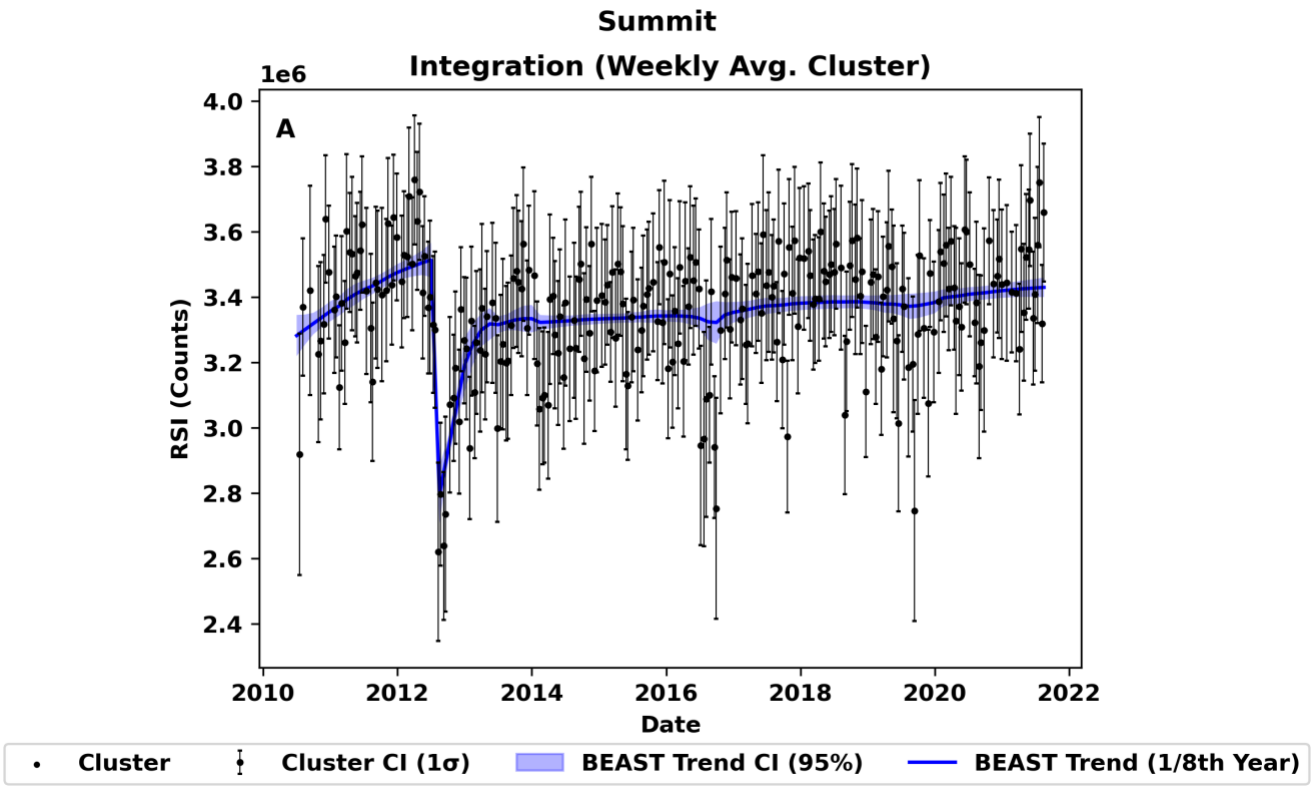

Figure 2A: RSI Trend at Summit Station

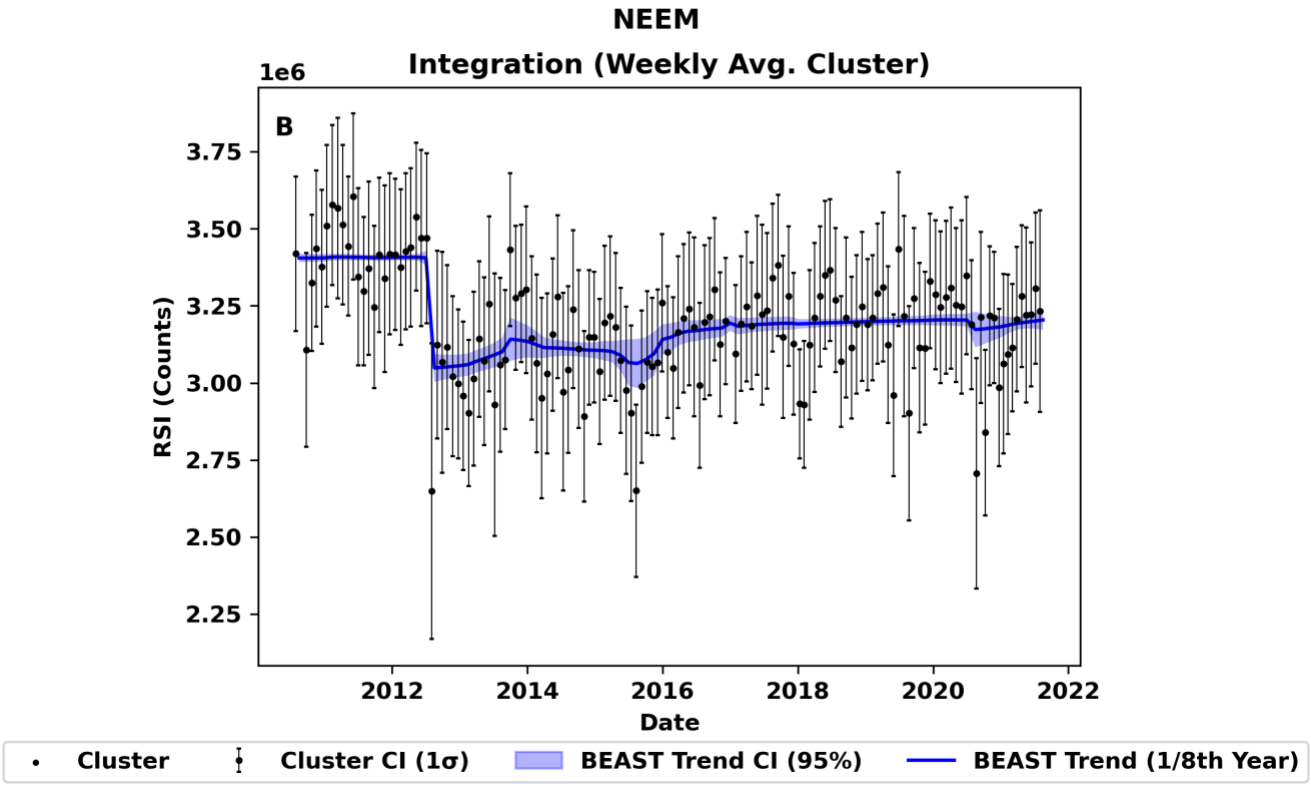

Figure 2B: RSI Trend at NEEM

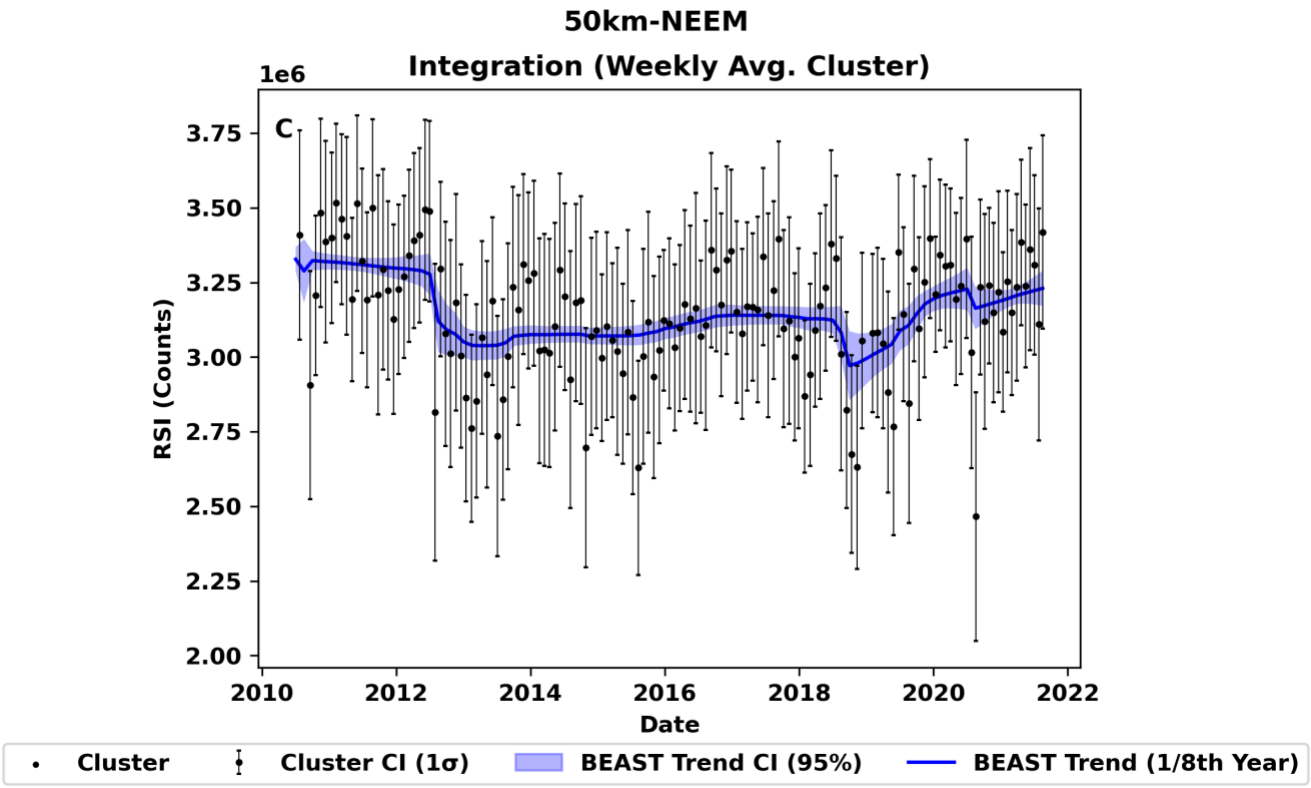

Figure 2C: RSI Trend at 50km-NEEM

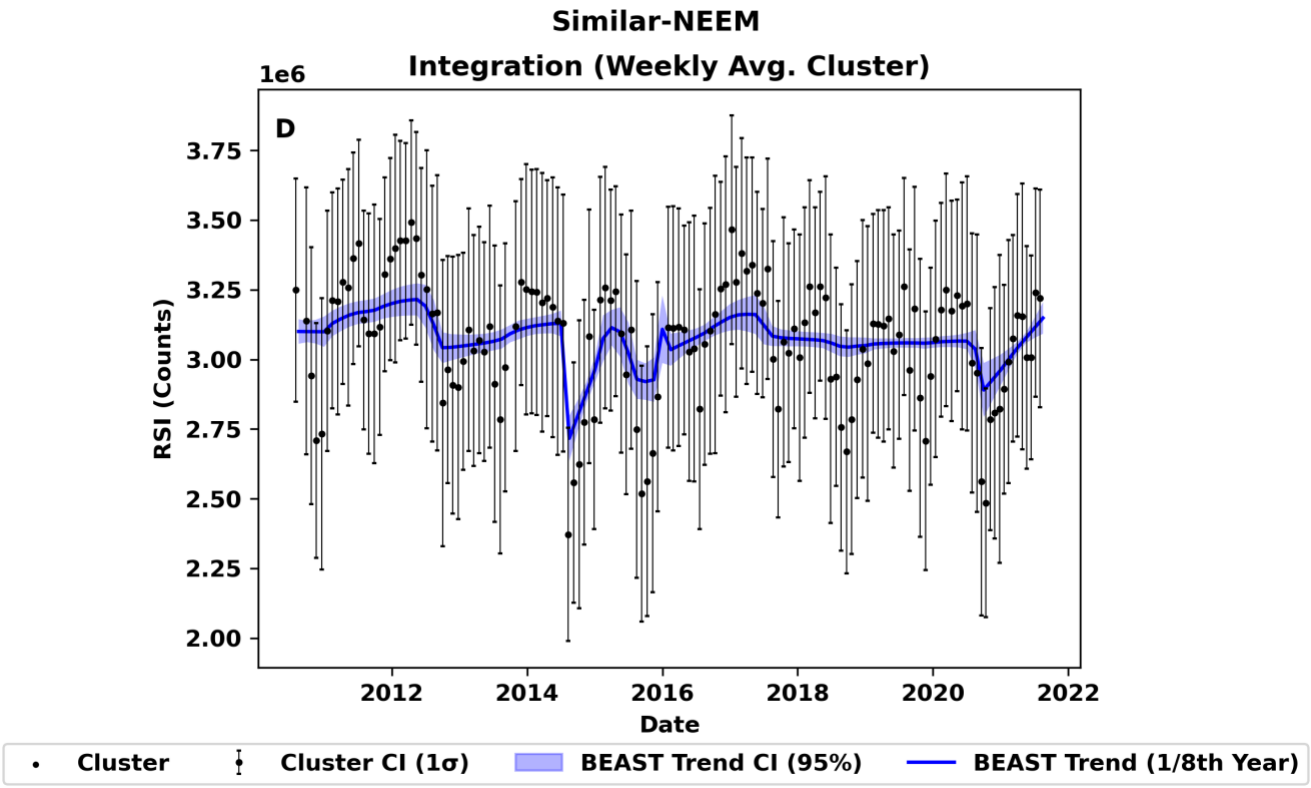

Figure 2D: RSI Trend at Similar-NEEM

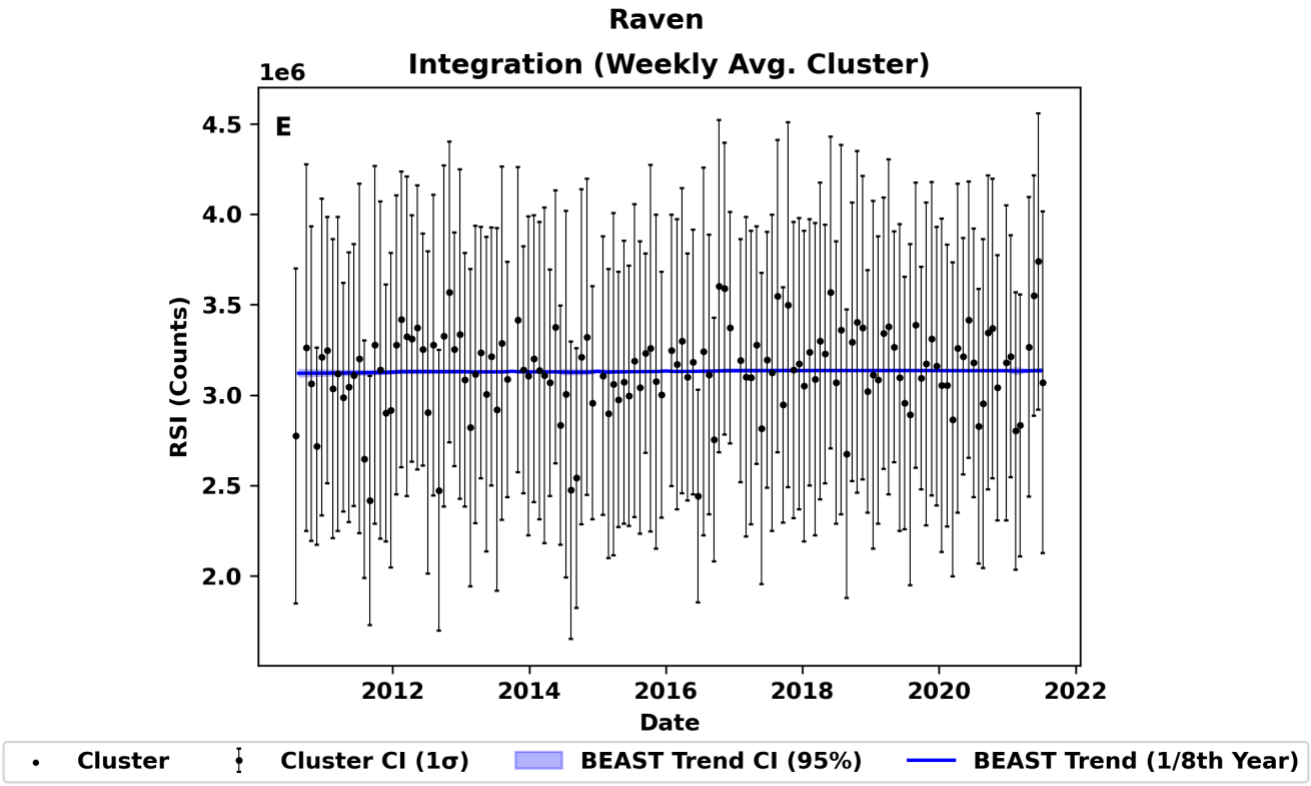

Figure 2E: RSI Trend at Raven

2.3 Trailing Edge Slope (TeS)

This study defines the TeS as the slope of best fit line of a least-squares linear regression during sections of maximum power drawdown. To determine what section of the waveform this corresponds to, this study makes use of where the maximum derivative in the latter half of the waveform corresponds to when the waveform tapers back towards baseline noise. The waveform is smoothed using a Savgol Filter (window length: 29, order: 2nd) and its derivative is calculated. The TeS is then calculated by applying a best-fit line through the range between the smoothed waveform's peak and the maximum value of the trailing edge smoothed-waveform derivative. We find no relationship between derived elevations and the Trailing Edge Slope, and no noticeable change over the duration of the time series (Figure 3A-E)

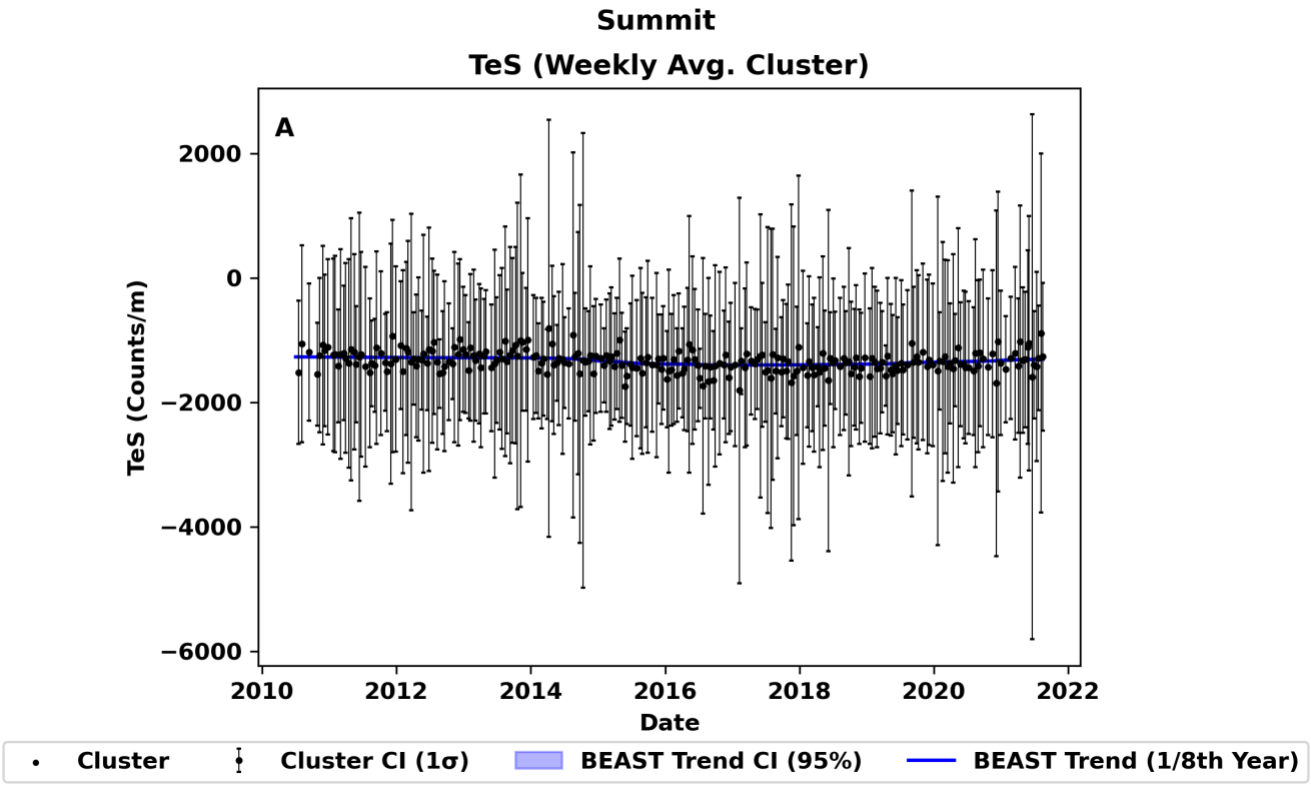

Figure 3A: TeS Trend at Summit Station

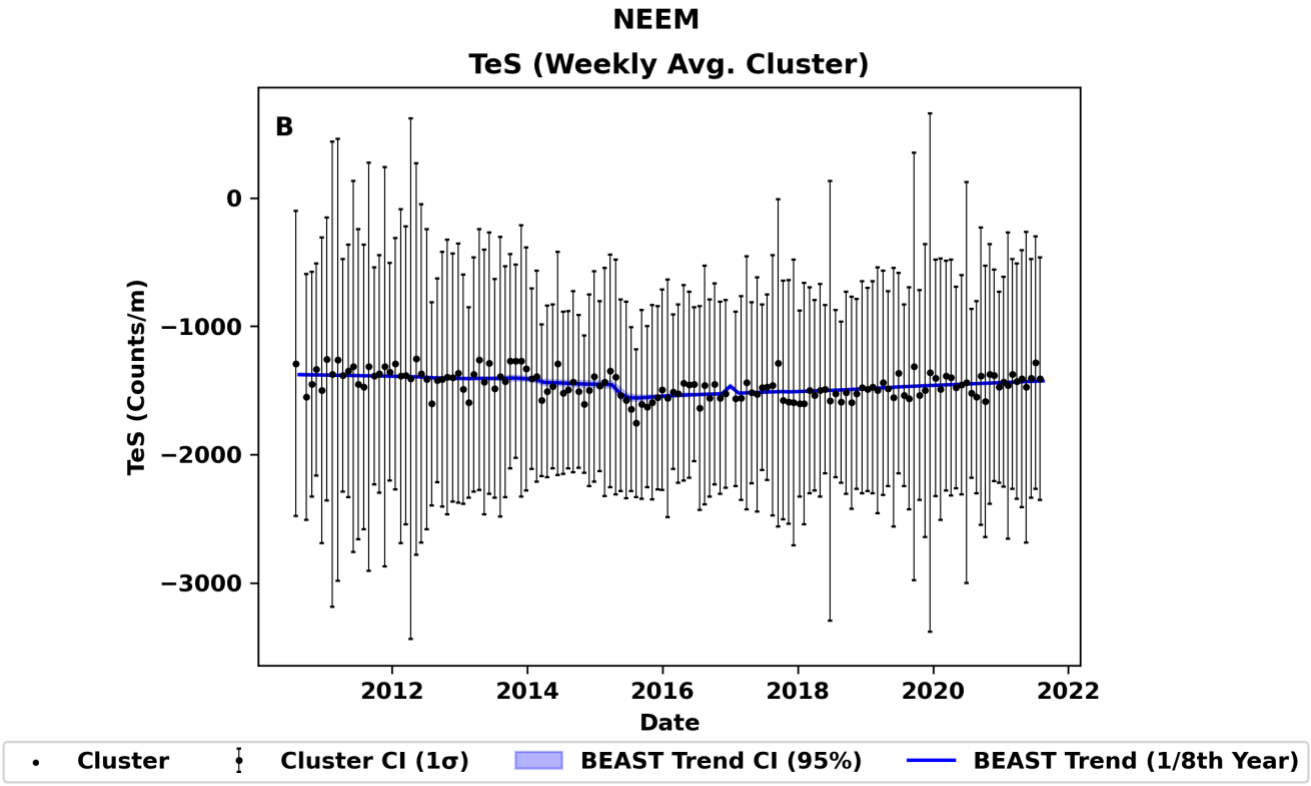

Figure 3B: TeS Trend at NEEM

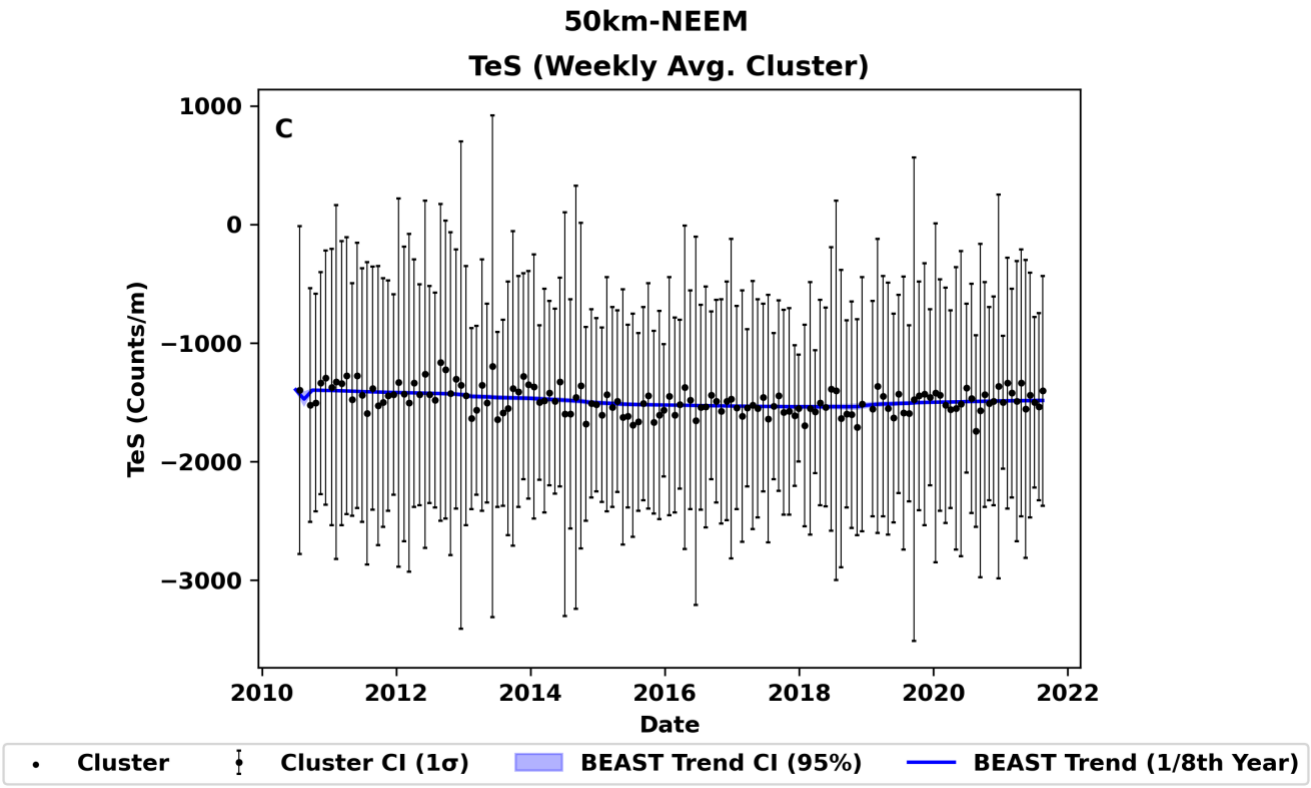

Figure 3C: TeS Trend at 50km-NEEM

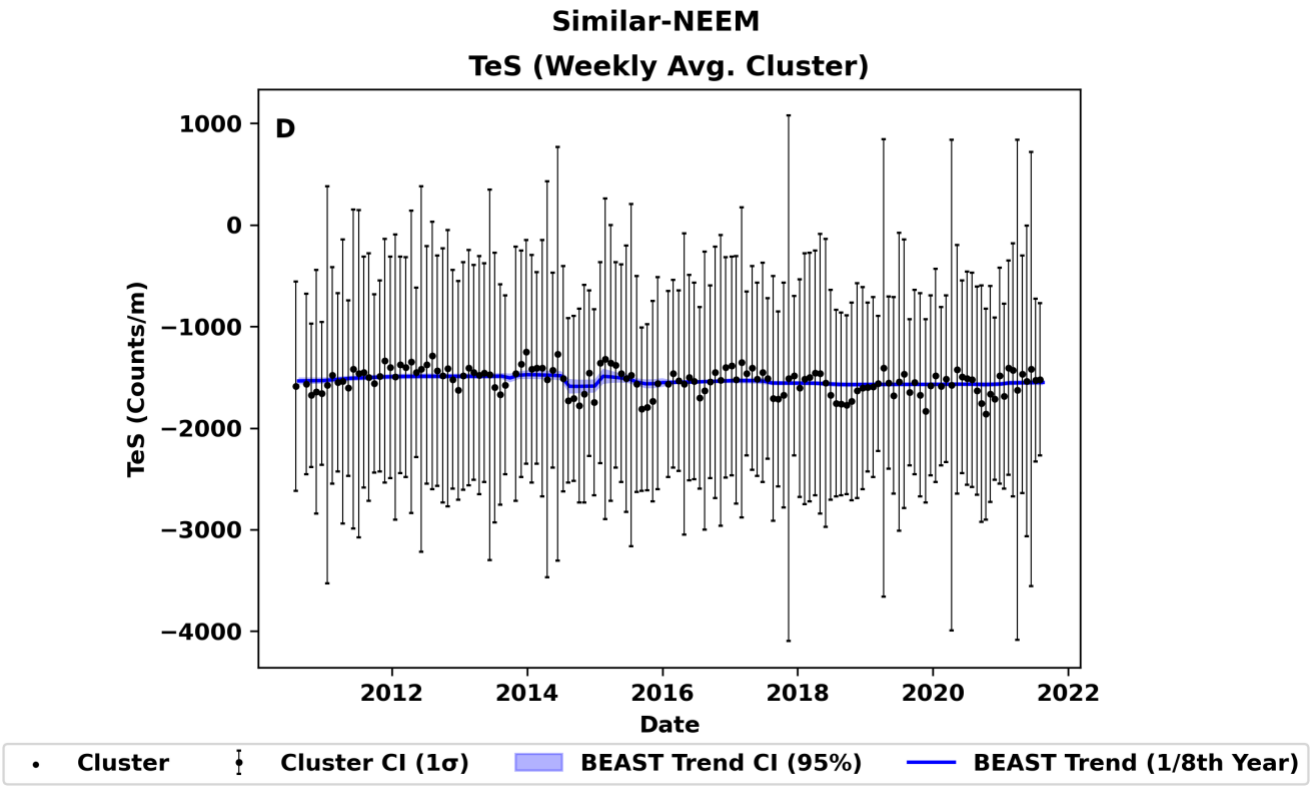

Figure 3D: TeS Trend at Similar-NEEM

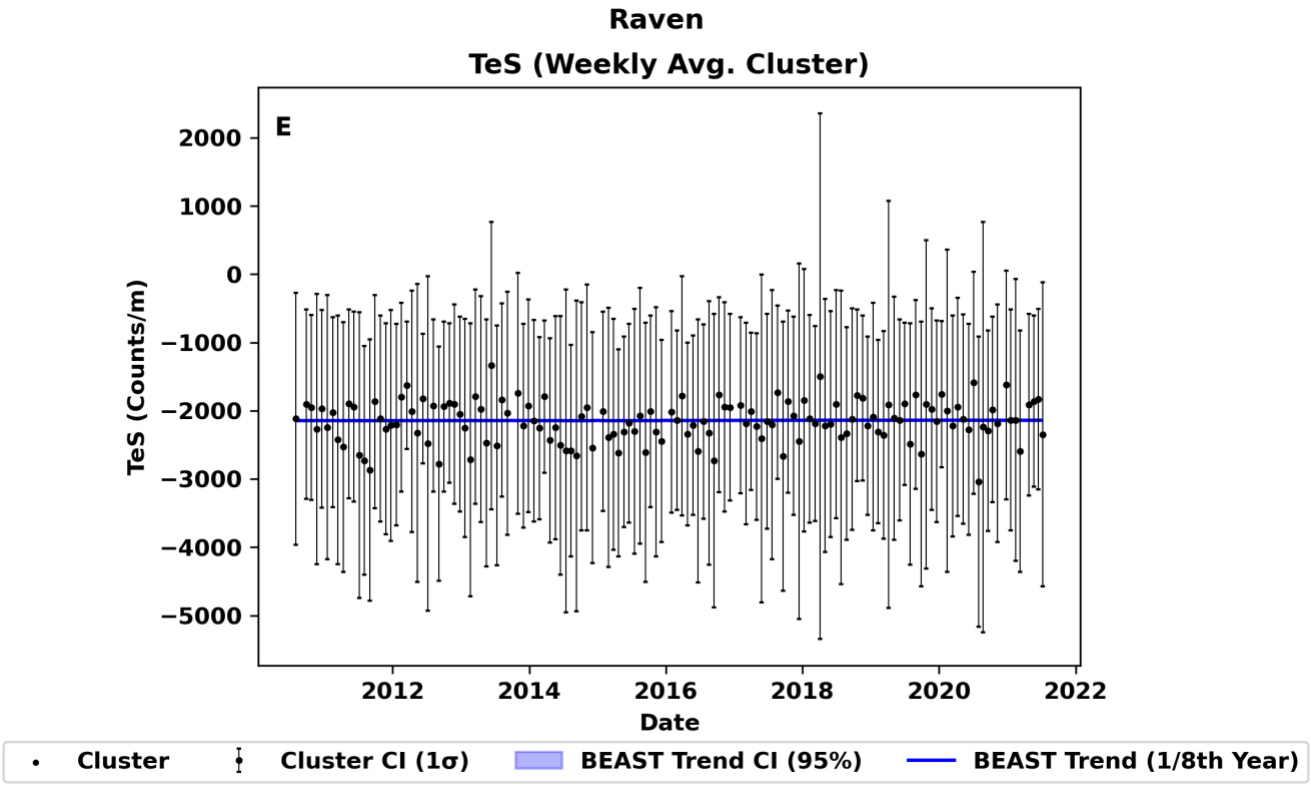

Figure 3E: TeS Trend at Raven

3.0 Elevation Plots

Here, we plot LeW with Level 2 ULI and OCOG Elevations for each site in the paper, as well as our additional sites. Though Summit, Neem, and Raven are all shown in the paper, we reproduce them here for completeness and for comparison with the additional two sites.

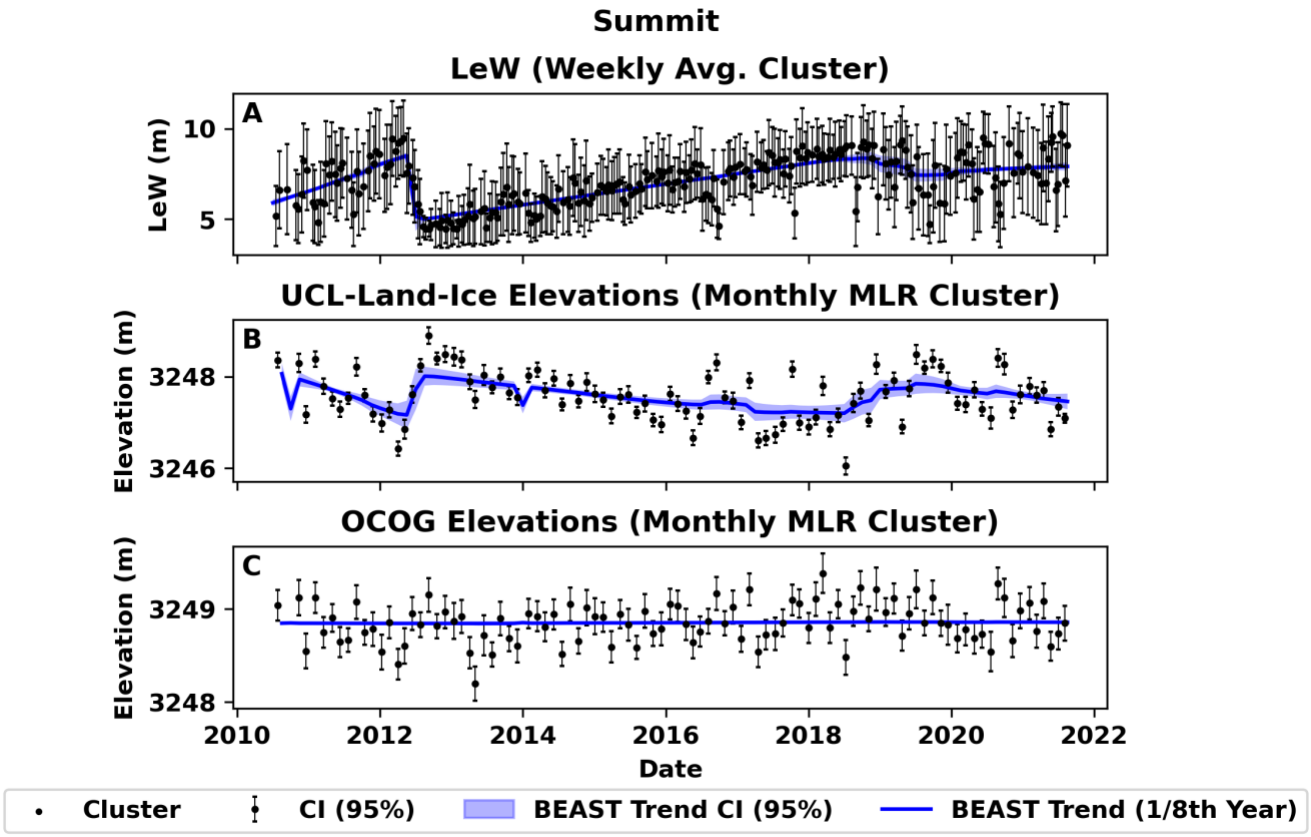

Figure 4: LeW and Level 2 ULI and OCOG Elevation Trends at Summit Station

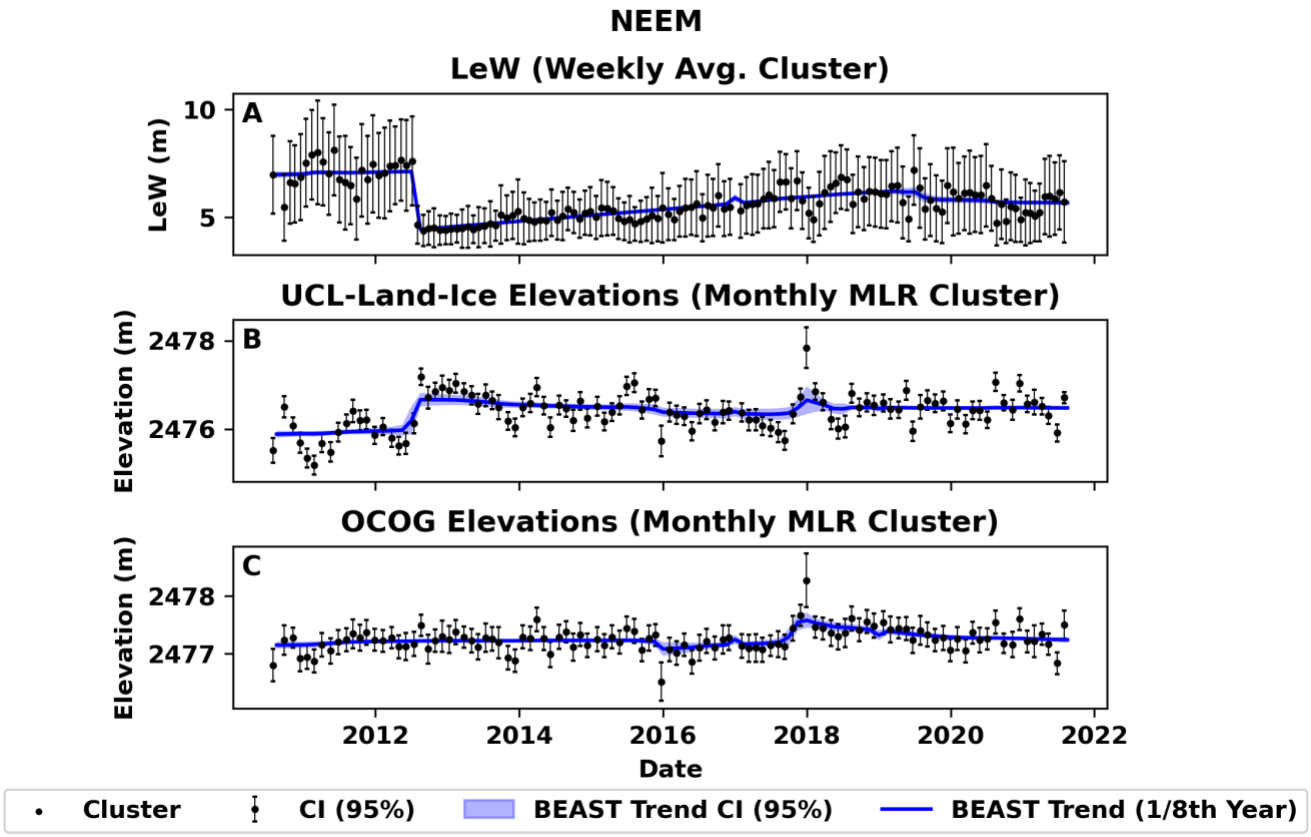

Figure 5: LeW and Level 2 ULI and OCOG Elevation Trends at NEEM

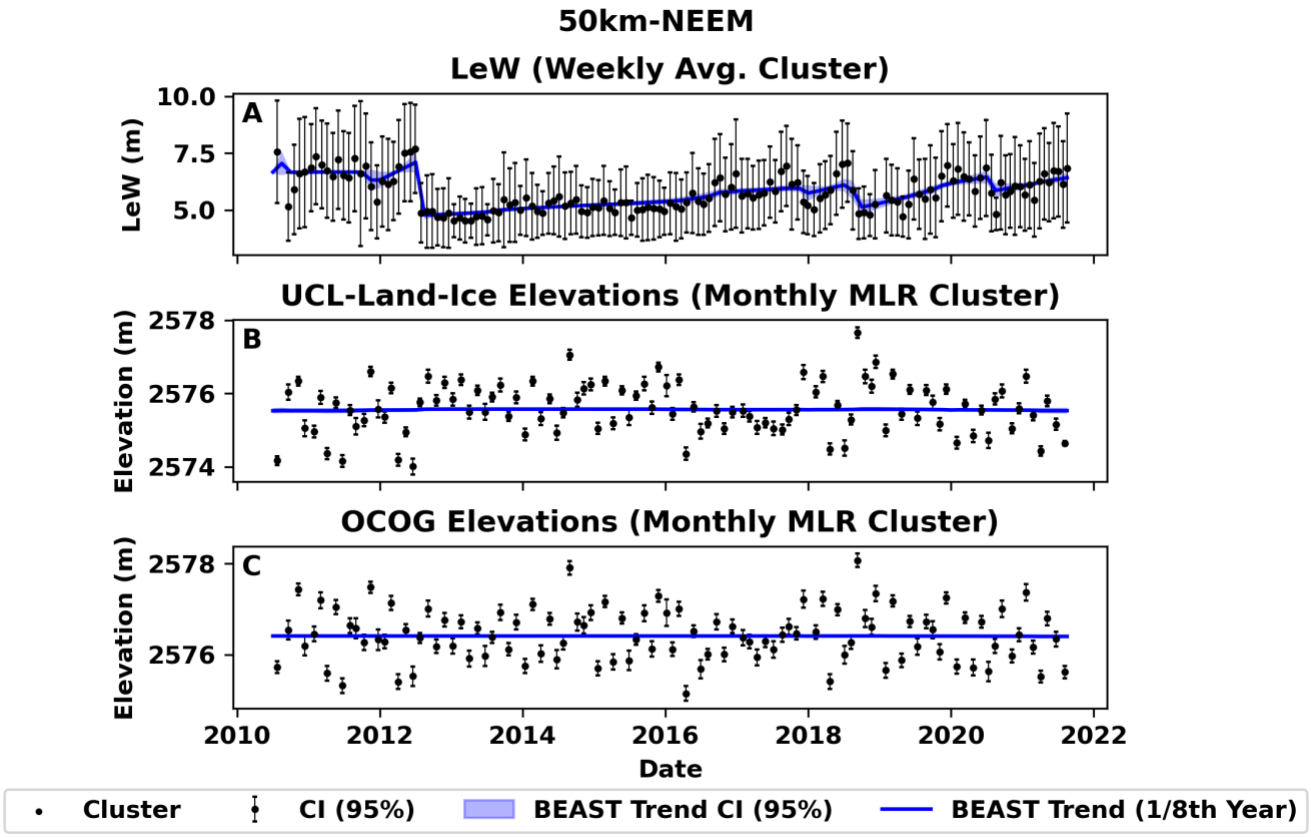

Figure 6: LeW and Level 2 ULI and OCOG Elevation Trends at 50km-NEEM

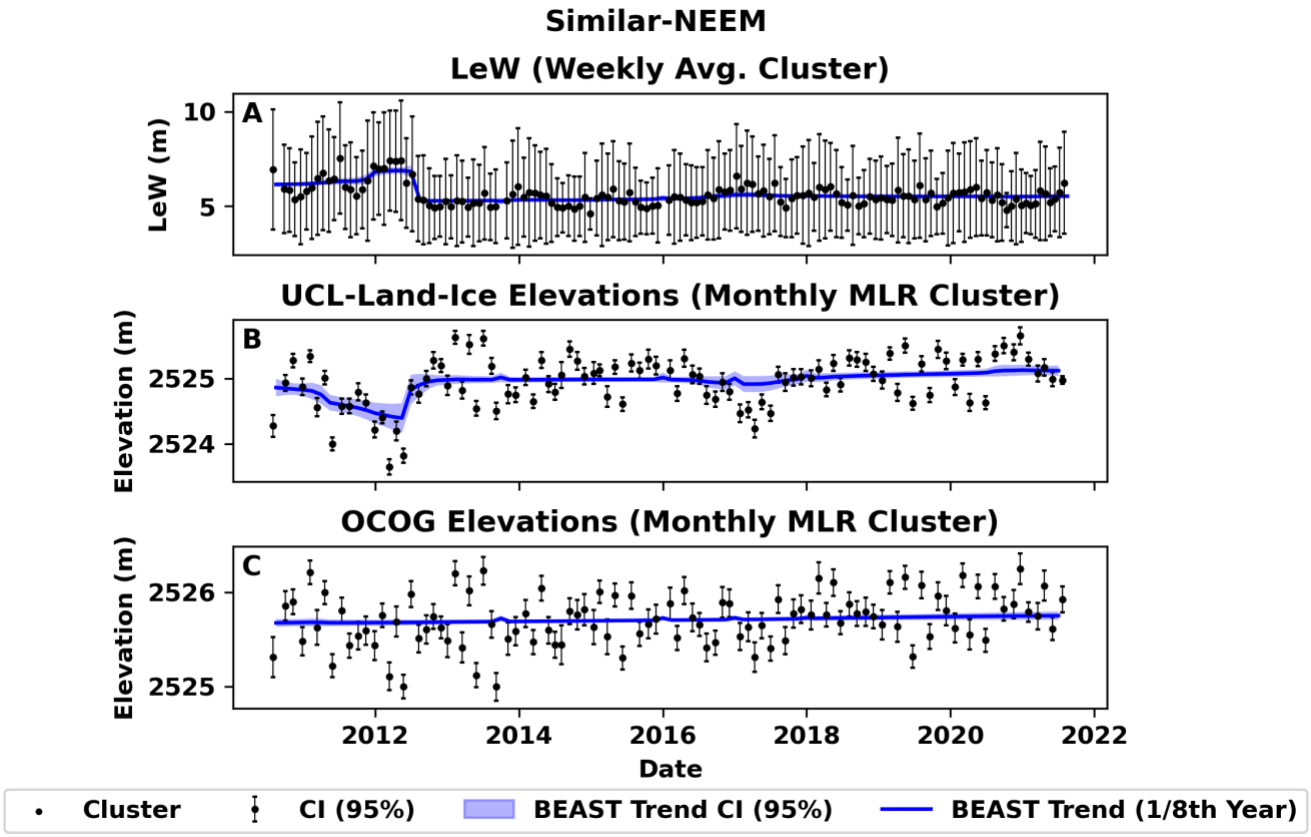

Figure 7: LeW and Level 2 ULI and OCOG Elevation Trends at Similar-NEEM

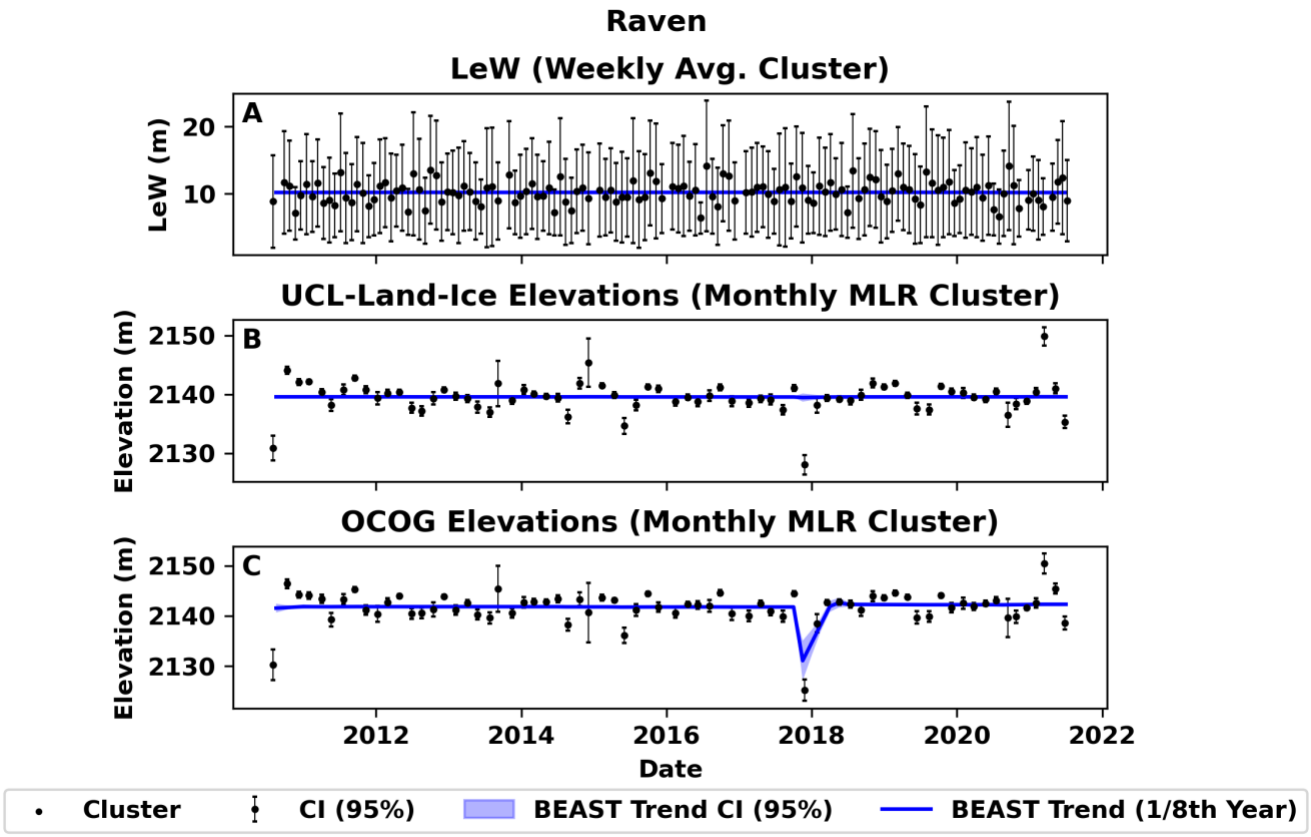

Figure 8: LeW and Level 2 ULI and OCOG Elevation Trends at Raven

4.0 Outliers

Level 1b waveforms that deviated from ideal were removed before the clustering and aggregation steps. Outliers were removed if the waveform array was incorrectly clipped and contained a second LeS after the TeS of the beginning, if they contained any Level 0, 1B, or Leap Error Flags, or contained irregularities that caused scripting error (Ronan et al., 2024). In addition, if the following conditions are met, a waveform is deemed as an outlier:

1. $LE \geq 64\ (Range\ Bins)$
    a. Explanation: When the leading-edge width of the clipped Level 1B waveform is greater than or equal to 64 range bins, corresponding to half the range bins of an un-clipped waveform.
    b. Purpose: Removes waveforms with abnormally large Les (Figure 9)

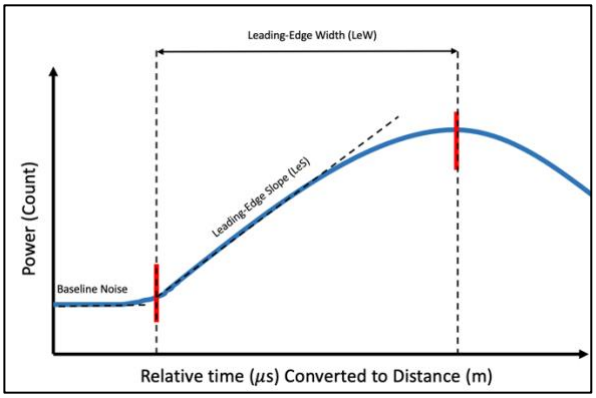

Figure 9: Illustration of Waveform with an abnormally large LE

2. $\frac{dy}{dx}(LE)\ \leq 500\ (\frac{Counts}{m})$
    a. Explanation: When any of the derivative values of the LE is below 500 Counts/m
    b. Purpose: Ensures only waveforms with straight LE (and waveform's with abnormally low LeS, Figure 9) are included, and those with a plateau (Figure 10) along the LE are not included.

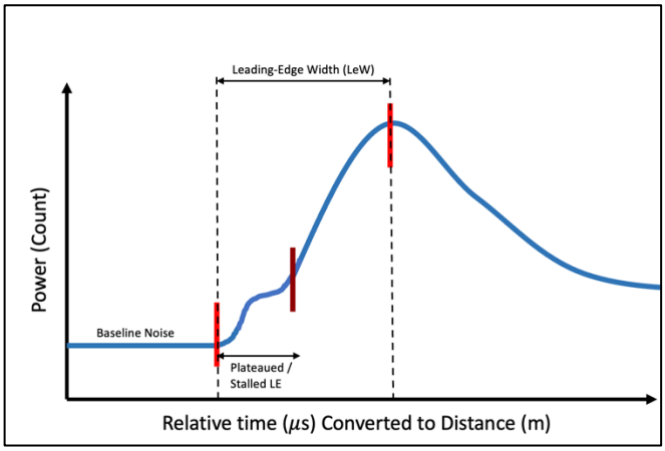

Figure 10: Illustration of Waveform with a plateaued LE

3. $\bar{X}_{S:Pre-LE} \geq \bar{X}_{R:Pre-LE} + 2\sigma_{\bar{x}_{R:Pre-LE}}$, where $\bar{X}_{S:Pre-LE}$ is the mean power of the selected waveform between eight and two positions before the beginning of the LE and $\bar{X}_{R:Pre-LE}$ is the mean power of the ideal waveform between eight and two positions before the beginning of the LE. $\bar{X}_{R:Pre-LE}$ is equivalent to [0, 137.8, 137.6, 363.8, 359.2, 1194]. This array was determined by empirically examining different "ideal" waveforms.
    c. Explanation: When the selected waveform's baseline noise floor is above two standard deviations of an "ideal" waveforms.
    d. Purpose: Ensures only waveforms with properly clipped LEs and baseline noise floors are included.

5.0. Climatology -LeW Plots

Plotting monthly averages of LeW yields no noticeable trend. These results are expected, given that we argue the LeW time series is not significantly altered by season, and is a function of a changing shallow subsurface.

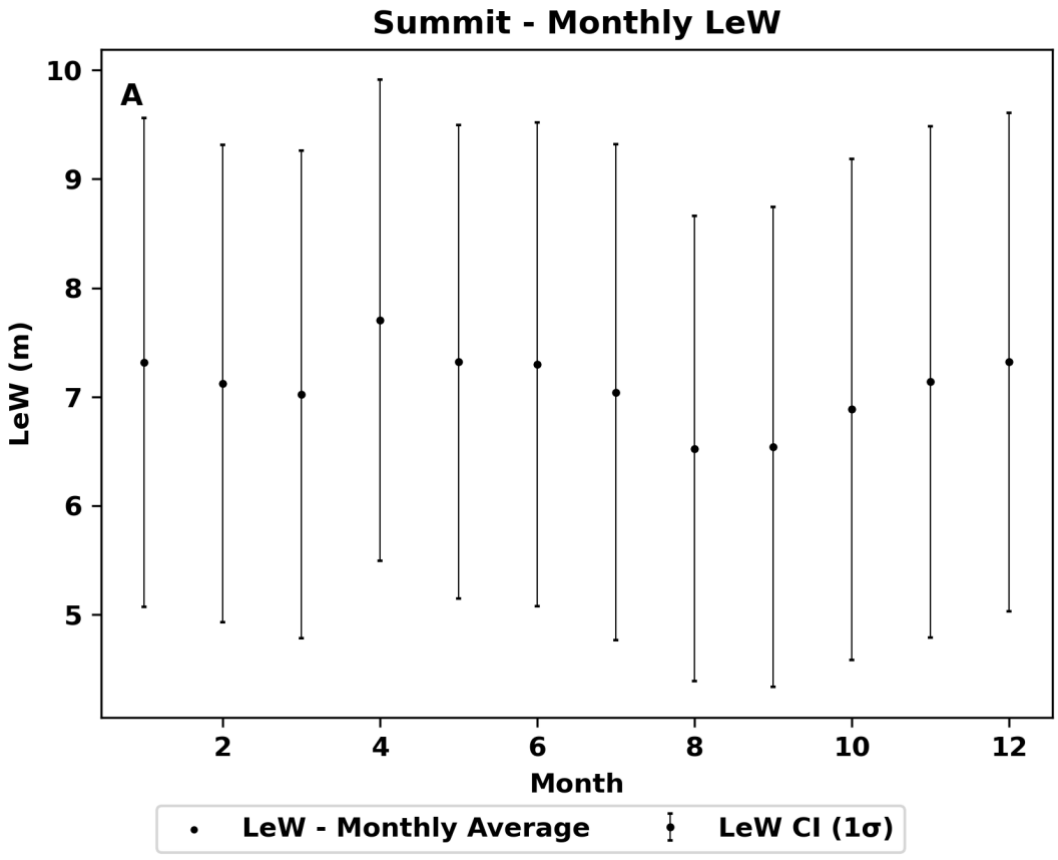

Figure 11A: Average LeW per month in the 2010-2021 time series at Summit Station

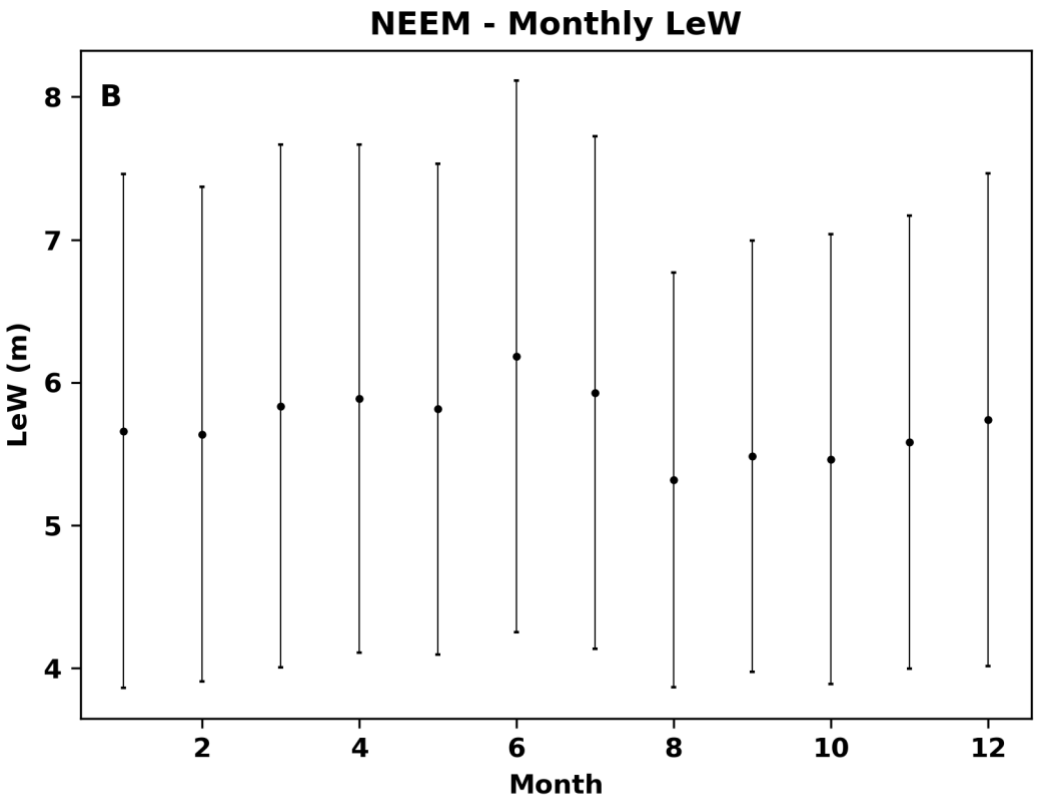

Figure 11B: Average LeW per month in the 2010-2021 time series at NEEM

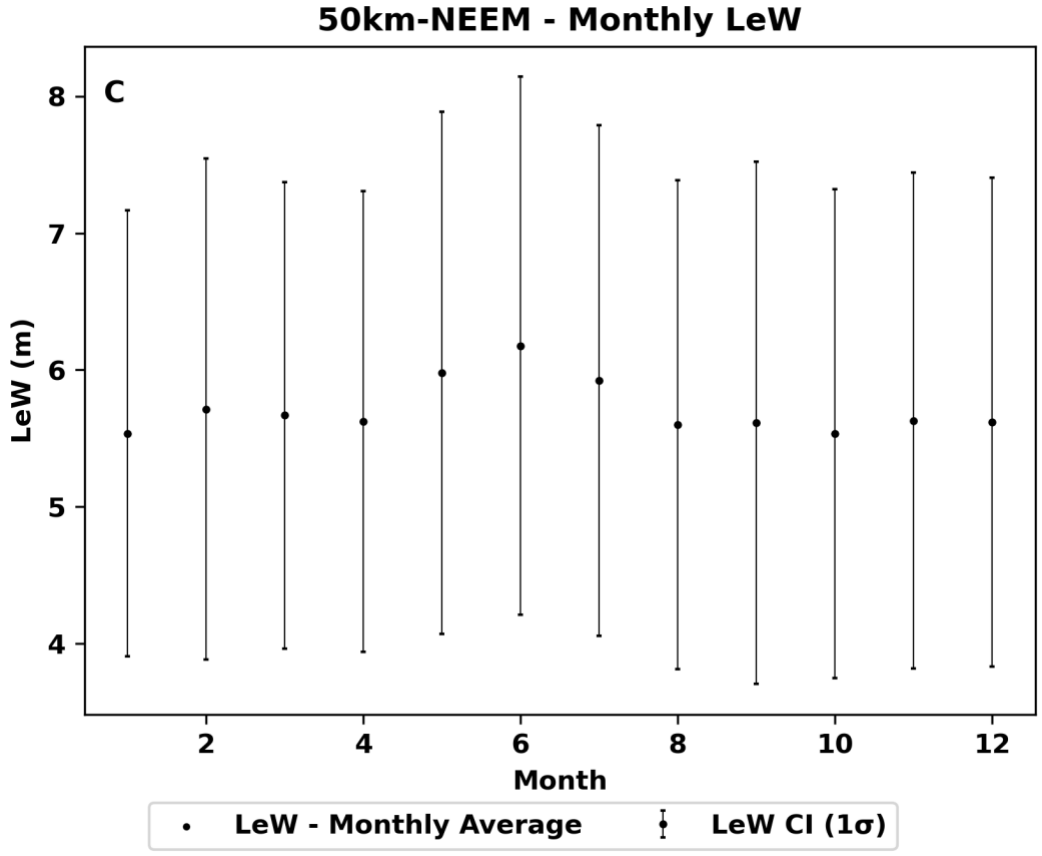

Figure 11C: Average LeW per month in the 2010-2021 time series at 50km-NEEM

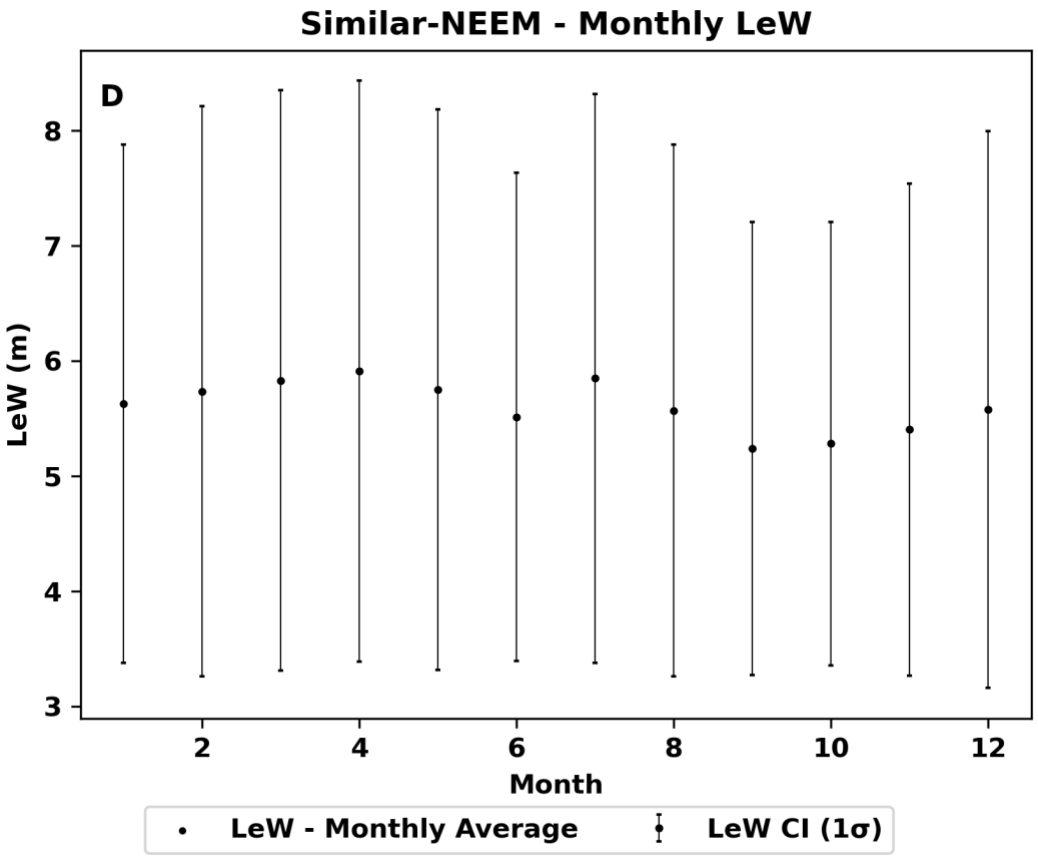

Figure 11D: Average LeW per month in the 2010-2021 time series at Similar-NEEM

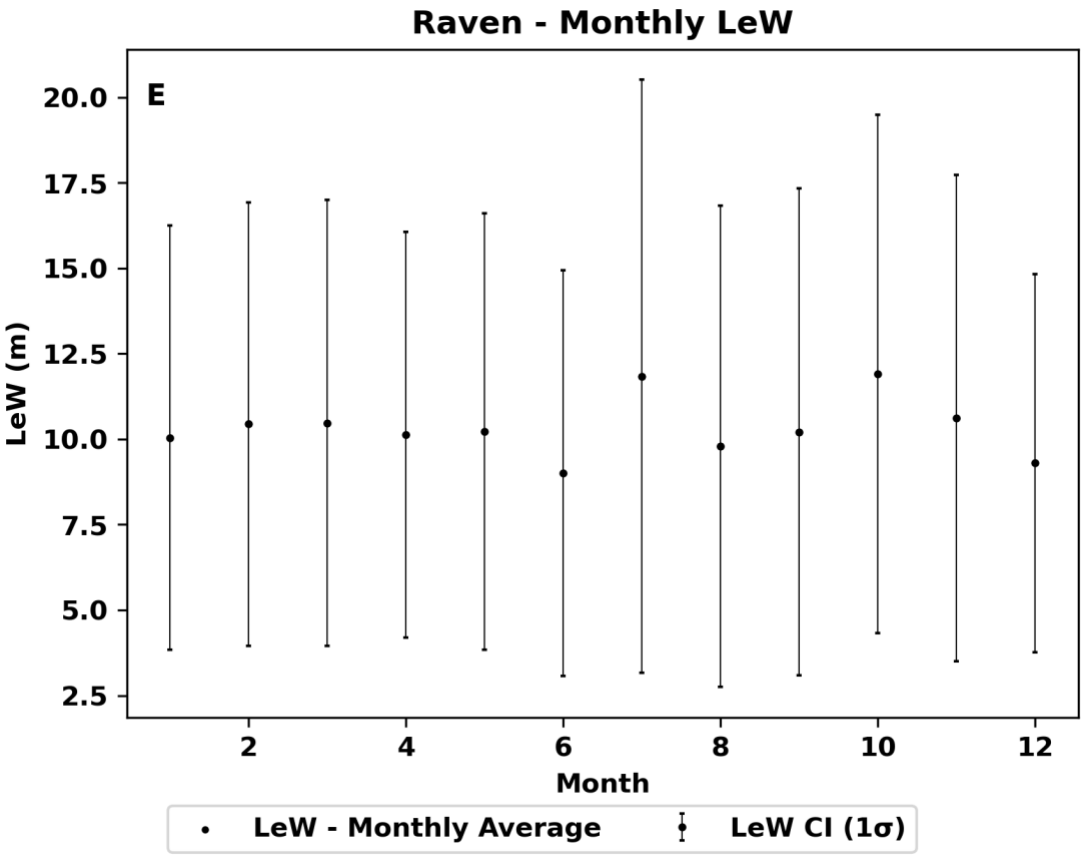

Figure 11E: Average LeW per month in the 2010-2021 time series at Raven

6.0 References

Dawson, G. J. and Landy, J. C.: Comparing elevation and backscatter retrievals from CryoSat-2 and ICESat-2 over
Arctic summer sea ice, Cryosphere, 17, 4165–4178, https://doi.org/10.5194/TC-17-4165-2023, 2023.

European Space Agency: CryoSat-2 L2 Design Summary Document,
https://earth.esa.int/eogateway/documents/20142/37627/CryoSat-2-L2-Design-Summary-Document.pdf,
last access: April 11, 2023, 2019

Howat, I., A. Negrete, and B. Smith. MEaSUREs Greenland Ice Mapping Project (GIMP) Digital Elevation Model,
Version 1.1. Boulder, Colorado USA. NASA National Snow and Ice Data Center Distributed Active Archive Center, [data set]. https://doi.org/10.5067/NV34YUIXLP9W, 2015.

Noël, B., van de Berg, W. J., Lhermitte, S., and van den Broeke, M. R.:
Rapid ablation zone expansion amplifies north Greenland mass loss, Sci Adv, 5,
https://doi.org/10.1126/SCIADV.AAW0123/SUPPL_FILE/AAW0123_SM.PDF, 2019.